HEAT TRANSFER CHARACTERISTICS OF ASSISTING AND OPPOSING LAMINAR FLOW THROUGH A VERTICAL CIRCULAR TUBE AT LOW REYNOLDS NUMBERS

Marilize Everts[1], Suvanjan Bhattacharyya[1,2], Abubakar I Bashir[1], Josua P Meyer[1*]

[1]Clean Energy Research Group, Department of Mechanical and Aeronautical Engineering, University of Pretoria, Pretoria, South Africa.

[2]Department of Mechanical Engineering, Birla Institute of Technology and Science, Pilani, Pilani Campus, Vidya Vihar, Rajasthan 333 031, India.

*Corresponding Author: josua.meyer@up.ac.za

HIGHLIGHTS

- Fully developed Nusselt numbers and correlations for assisting and opposing flow.
- Forced convection conditions existed for Reynolds numbers greater than 600.
- Nusselt numbers of assisting and opposing flow increased with Reynolds number.
- Increased heat flux leads to assisting flow at lower Reynolds numbers.
- Increased heat flux leads to opposing flow at higher Reynolds numbers.

ABSTRACT

Owing to its importance in industrial applications, many studies investigated mixed convective flow through vertical tubes. These studies usually considered tubes with relatively large diameters and short lengths. The result was that the flow was developing rather than fully developed, which affects the heat transfer characteristics and free convection effects. The purpose of this study was therefore to consider fully developed upward and downward flow at very low laminar Reynolds numbers in forced convection conditions and to investigate the heat transfer characteristics when assisting and opposing flow became significant due to the low fluid velocities. Experiments and numerical simulations were conducted for vertically upward and downward flow between Reynolds numbers of 180 and 2 300 at three different heat fluxes of 1, 1.5 and 2 kW/m^2. Water was used as the test fluid and the Prandtl numbers varied between 3 and 7. The inner-tube diameter was 5.1 mm and the heated length-to-diameter ratio was 886. It was found that as the Reynolds number was decreased below 250 and 600 for upward and downward flow, respectively, free convection effects were no longer suppressed by the velocity of the fluid and assisting and opposing flow became significant. The Nusselt numbers of upward flow were always greater than for downward flow. Increasing free convection effects caused both the upward and downward results to shift further from the forced convection

Nusselt numbers. Correlations were developed to determine the Nusselt numbers for assisting and opposing laminar flow.

Keywords: heat transfer; laminar flow; vertical tube; Nusselt number; opposing; assisting

Nomenclature

C_p	Specific heat at constant pressure
D	Diameter
DAQ	Data acquisition system
DC	Direct current
eb	Energy balance error
g	Gravitational acceleration
Gr	Grashof number
h	Heat transfer coefficient
I	Current
i	Data point index
k	Thermal conductivity
L	Length
Lt	Thermal entrance length
$\dot{m}$	Mass flow rate
Nu	Nusselt number
P	Static pressure
Pr	Prandtl number
$\dot{Q}$	Heat transfer rate
$\dot{q}$	Heat flux
R	Radius
r	Radial direction
Re	Reynolds number
T	Temperature
u	Velocity in axial direction
V	Voltage/Velocity
x	Distance from tube inlet

Special characters

β	Coefficient of thermal expansion
μ	Dynamic viscosity
ρ	Density

Subscripts

avg	Average
b	Bulk
f	Fluid
FD	Fully developed
i	Inlet/inner/axial direction
j	Radial direction
o	Outlet
s	Surface

1. Introduction

Heat exchangers have a wide range of applications, such as solar receiver tubes, air-conditioning and refrigeration systems, cooling of electronic equipment and power generation plants operated by fossil fuels, nuclear or concentrated solar power. Owing to the high heat transfer coefficients associated with turbulent flow, heat exchangers are usually designed to operate in this flow regime. However, changes in operating conditions, operational transients or accidents, system upgrades, design constraints, and fouling, can cause heat exchangers to operate in the transitional or even laminar flow regimes.

To avoid freezing, fluids other than water, such as glycols, are often used in heat exchangers that operate in very cold climates. As the viscosity of these fluids are usually significantly higher compared to that of water, the pump flow rate is decreased to reduce high pressure drops and thus operational running cost, which causes the heat exchangers to operate in the laminar or transitional flow regime. In the recent years, there has also been a growing interest in heat exchangers that consist of mini-tubes, rather than macro-tubes. The interest in shift to compact heat exchangers started because these heat exchangers occupy less space, require less material, as well as less heat exchanger fluids [1]. It should, however, be noted these compact heat exchangers are also likely to operate in the laminar flow regime, due to the reduced flow rates through the small hydraulic diameters compared to macro systems. In order to design and optimise efficient heat exchangers, it is therefore important to have accurate heat transfer correlations not only for turbulent flow, but also laminar and transitional flow.

According to most authoritative heat transfer books [2-7] the Nusselt number is 4.36 for fully developed laminar flow through a tube with a constant heat flux boundary condition. Furthermore, it is also reported that the Nusselt number remains constant irrespective of variations in Reynolds number, Prandtl number, axial tube position or orientation of the heat exchanger. This constant Nusselt number of 4.36 could be attributed to the assumption of constant fluid properties such as density, viscosity, thermal conductivity and specific heat in the Nusselt number derivation. Because, almost all heat transfer fluid and gas properties are a function of temperature, temperature gradients exist in the heat transfer fluids and gases of almost all heat exchangers and these temperature differences lead to density differences and thus free convection effects in the presence of gravity.

Although these free convection effects are always present, it can either be significant or negligible in comparison to the forced convection heat transfer due to the pump or fan. When free convection effects are negligible, the flow is dominated by forced convection. However, when free convection effects are significant, the flow is dominated by mixed convection. Three different situations exist in mixed convection conditions. Depending on the orientation of the heat exchanger and the direction of the flow, free convection effects can either be in the same direction (assisting flow), opposite direction (opposing flow) or perpendicular (secondary flow) to the direction of the forced flow.

Previous studies [8-11] that experimentally investigated mixed convective flow, found that the Nusselt numbers were easily around 180% to 520% greater than 4.36 for horizontal tubes. For

vertical tubes, an increase in Nusselt number of 30% to 220% was observed [12, 13]. In order to optimise the design of heat transfer equipment, it is therefore important to know whether free convection effects can be neglected or not, because this will determine whether forced or mixed convection design correlations should be used.

A flow regime map is a valuable tool to determine whether free convection effects are significant or not. Metais and Eckert [14] developed flow regime maps for vertical tubes with either a constant heat flux or a constant surface temperature boundary condition, as well as for horizontal tubes with a constant surface temperature boundary condition. Everts and Meyer [15] recently developed flow regime maps for horizontal tubes heated at a constant heat flux. Although mixed convection conditions are commonly accepted for Richardson numbers between 1 and 10, care should be taken when using this criterion, because it was developed for upward flow along a vertical flat heated plate, while mixed convection effects through tubes are more complex [16].

Meyer and Everts [10] found in their study using horizontal tubes, that mixed convection conditions existed in 95% of their 891 fully developed laminar experimental data points. Similar to Newell [17], Meyer and Everts [10] concluded that forced convection conditions could only be obtained when small diameter test sections or very small heat fluxes were used. Although mixed convection conditions exist in most applications, and accurate mixed convective heat transfer correlations are vital for the optimisation of heat transfer equipment, mixed convection heat transfer receives surprisingly little attention in heat transfer textbooks [18]. While most textbooks devote separate chapters to forced and natural convection, many textbooks only devote a couple of pages to mixed convection. Possible reasons for this might be the complexity of mixed convective flows and the contradicting results reported in literature [18].

However, owing to its importance in industrial applications, many studies investigated mixed convective flow through vertical tubes. Jackson *et al*. [19] gives a comprehensive review of the work done on mixed convective flow using vertical tubes between 1942 and 1989, while Galanis and Behzadmehr [18] reviewed the work done between 1988 and 2008. For vertical tubes heated at a constant heat flux, several analytical [20-23], experimental [1, 12, 13, 23-31] and numerical [25, 32-38] studies investigated the heat transfer characteristics.

In general, it was found that for assisting flow (upward flow in heated tubes), the density of the fluid near the surface of the tube decreased due to the increased temperature, which caused the fluid to rise. The upward motion due to free convection effects, combined with the upward forced motion (due to the pump or fan) caused the fluid near the surface of the tube to accelerate. To satisfy continuity, the colder fluid (with a higher density) near the centre of the tube was pushed downward. This downward trend combined with the upward forced flow, caused the fluid in the centre of the tube to slow down. The increased velocity of the fluid near the surface of the tube, assisted in distributing the heat from the surface to the centre of the tube. The result was enhanced heat transfer and thus higher heat transfer coefficients than in the absence of any free convection effects. On the other hand, for opposing flow (downward

flow in heated tubes), the fluid near the tube wall was slowed down, because free convection effects acted in the opposite direction as the forced flow. This resulted in impaired heat transfer and lower heat transfer coefficients than in the absence of any free convection effects.

Because these studies focussed specifically on opposing and assisting flow in mixed convection conditions, the heat transfer coefficients were significantly affected by free convection effects and the direction of the flow. Previous studies that focused on inclined tubes [22, 26, 31, 33, 34, 39] found that free convection effects significantly decreased as the orientation of the heat exchanger was changed from horizontal to vertical. Bashir *et al*. [40] also found that when vertical tubes are used, forced convection conditions could be obtained at heat fluxes as high as 8 kW/m^2 for both assisting and opposing flow for laminar Reynolds numbers greater than 1 000. This heat flux was eight times more than the heat flux that could be applied to obtain forced convection conditions in the same test section, but in a horizontal position. As forced convection conditions existed, there was a negligible difference between the Nusselt numbers of opposing and assisting flow, and the Nusselt number results as a function of Reynolds number collapsed onto a single line. This is in contrast to the results in literature on flow through heated vertical tubes [1, 12, 13, 20-38]. A possible reason for this significant difference in trends might be due to the dimensions of the tubes that were investigated.

In literature [1, 12, 13, 23-31], vertical flow experiments were conducted using test sections with maximum length-to-diameter ratios (L/D_i) that varied between 23 and 138, except for two test sections of Kemeny and Somers [12] that had maximum length-to-diameter ratios of 200 and 400. Bashir *et al*. [40] conducted experiments using a test section with a maximum length-to-diameter ratio of 886. This ratio was thus approximately 2-39 times more than what has been used in the past. Mohammed and Yusaf [26] concluded when using their test section of $L/D_i = 30$ that, especially for downward flow, the secondary flow loop caused by free convection effects most probably extended across the entire tube length, which prevented the flow from becoming fully developed. Lawrence and Chato [32], who investigated both upward and downward flow, also concluded that free convection effects caused the velocity and temperature profiles to change continuously and therefore prevented the flow from becoming fully developed. Because the heat transfer coefficients of developing flow are generally higher than for fully developed flow, this might be the reason why the Nusselt numbers were affected significantly by upward and downward flow.

A general trend in literature was that free convection effects (thus Grashof number) caused an increase in Nusselt number, but developing flow might have played a dominant role in this increase. For the slender tube ($L/D_i = 886$) of Bashir *et al.* [40], the secondary flow loop could not extend across the entire tube length. Therefore free convection effects were less compared to the shorter test sections used in previous investigations [1, 12, 13, 23-31]. For their range of Reynolds numbers greater than 1 000, free convection effects were therefore suppressed for vertical flow. This, however, might change if the Reynolds number is decreased well below 1 000 and free convection effects become significant compared to the very low forced flow velocities.

Owing to its importance in industrial applications, correlations to predict the heat transfer coefficients of vertical opposing and assisting flow in mixed convection conditions exist in literature [1, 26, 29, 30], but they are limited to very specific conditions [41]. As these correlations were developed for mixed convection conditions using tubes in which the flow could not become fully developed, they are mainly functions of Grashof number (or Rayleigh number) and Graetz number. The correlations were also developed from experimental data obtained using a specific test fluid such as air [26, 29], water [30] and water based SiO_2 nanofluids. The Prandtl number range, which affects both the Rayleigh number and Graetz number, is thus very limited. Furthermore, Su and Chung [36] found that the Prandtl number has a significant effect on the free convection effects that may lead to flow instabilities, especially for assisting flow.

For forced convection conditions, Bashir *et al*. [40] developed an accurate fully developed flow laminar Nusselt number correlation for Reynolds numbers greater than 600. The authors showed experimentally using a vertical tube that the Nusselt numbers were constant at 4.36 for Reynolds numbers between 600 and 1 000, but became a function of Reynolds number as the Reynolds number was increased above 1 000. They also recommended that experiments be conducted at lower Reynolds numbers (because they observed signs of assisting and opposing flow becoming significant at a Reynolds number of 600). When the flow is fully developed and the Reynolds number (and thus fluid velocity) is decreased significantly in forced convection conditions, free convection effects may become significant and therefore influence the heat transfer characteristics.

The purpose of this study was therefore to experimentally and numerically investigate the heat transfer characteristics of assisting and opposing fully developed laminar flow in vertical tubes at low laminar Reynolds numbers. Unlike previous investigations in literature, the length of the test section was sufficient for the flow to be fully developed and forced convection conditions existed. Furthermore, for a detailed investigation and understanding of the characteristics of assisting and opposing flow, temperature and velocity profiles were obtained by numerical computations, using ANSYS Fluent, and compared and validated with the experimental data. Correlations were also developed to determine the heat transfer coefficients of assisting and opposing flow at low laminar Reynolds numbers.

2. Experimental set-up

The experimental set-up and procedure are fully reported in Meyer *et al*. [39], but for the sake of completeness, it is summarised in this paper. The experimental set-up (Fig. 1) consisted of a closed fluid loop, flow-calming section, inlet section, test section and test bench structure. Water was used as the test fluid and a chiller unit was coupled to the storage tank to cool down the heated water and also to maintain the water at a constant temperature. A Coriolis mass flow meter with an accuracy of 0.05% of the full scale (108 ℓ/hr) was used to measure the mass flow rates. The pump and Coriolis mass flow meter combination limited the minimum mass flow rate of this experimental set-up to a Reynolds number of 180.

Fig. 2 is a schematic of the test section indicating the thermocouple stations. The test section was made from a smooth hard-drawn copper tube with an inner and an outer diameter of 5.1 mm and 6.3 mm, respectively. It had a total length of 4.6 m, which gave a maximum length-to-diameter ratio (x/D_i) of 886. The test section was placed onto a 6 m long rigid frame with a height of 3 m. The test bench was pivoted at the centre in such a way that the water could flow through the test section in either a vertical upward or downward direction.

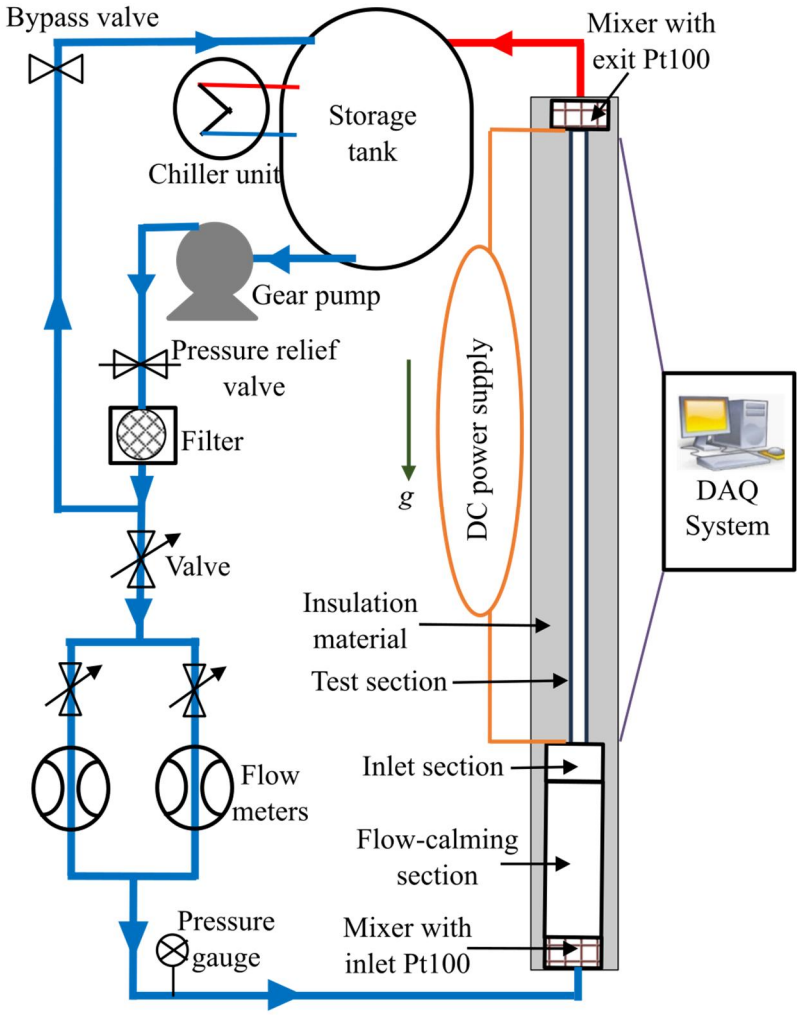

Fig. 1: Schematic of the experimental set-up with flow in the upward direction. Figure taken from Bashir *et al.* [40].

The wall temperatures were measured at 21 thermocouple stations and the thermocouple stations were located at closer intervals near the entrance, as well as in the fully developed region, to capture enough data in these regions. Copper-constantan T-type thermocouples with a diameter of 0.25 mm were soldered to the outside of the tube. Three thermocouples were used at each station with one at the top (0°), one at the bottom (180°), and a third thermocouple alternating at the side between 90° (for stations 1, 3, 5 etc.) and 270° (for stations 2, 4, 6 etc.).

The theoretical forced convection thermal entrance length, L_t, was calculated to be 3 m based on $Lt = 0.05RePrD_i$ for a Reynolds number of 2 100 and Prandtl number of 6. Conservatively,

the last 1.6 m of the test section always had fully developed flow. However, recent work [10, 42] showed that $Lt = 0.12RePrD_i$ when the flow is simultaneously hydrodynamically and thermally developing, as in this study. Unfortunately, this experimental set-up and test section was built before this thermal entrance length results were obtained. It would have been more correct to use a test section with a total length of 8 m (7 m for the flow to become fully developed and the last 1 m for the fully developed flow measurements). However, Fig. 5 in Everts and Meyer [42] indicate that the difference in Nusselt number when using coefficients of 0.05 and 0.12 is only approximately 5%. Furthermore, this study specifically focussed on assisting and opposing flow, which occur at Reynolds numbers less than 600. For these conditions, the thermal entrance length is less than 2.2 m. For these reasons, the results in this study were considered as fully developed and valid. The "fully developed" part of the test section in Fig. 2 was used to obtain the fully developed heat transfer results.

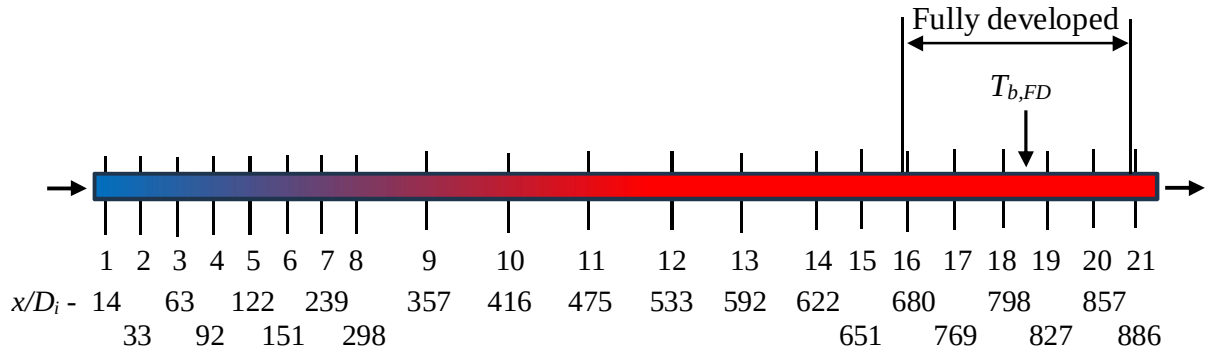

Fig. 2: Schematic of the test section indicating the thermocouple stations. Figure adapted from Meyer *et al.* [39].

To obtain a constant heat flux boundary condition, two constantan heating wires, with diameters of 0.38 mm, were tightly coiled around the test section (skipping the thermocouple junctions) and were connected in parallel to a DC power supply. Three different heat fluxes of 1, 1.5, and 2 kW/m^2 were investigated in this study. These fairly low heat fluxes that are relatively close to each other were due to the limitations of the experimental set-up, as well as the focus of this study. As the thermocouples were soldered onto the test section, the surface temperatures were kept below 90 °C, because the solder would start to melt at temperatures above 90 °C. The maximum surface outlet temperatures were limited to approximately 60 °C, the maximum recommended operational material temperature of some of the fittings and tubes downstream of the test section. Therefore, to ensure that the surface and fluid temperatures at the outlet of the test section did not exceed 90 °C and 60 °C, respectively, at the minimum Reynolds number of 180, the heat flux was limited to 2 kW/m^2. Furthermore, the heat flux was not reduced below 1 kW/m^2 to ensure that the surface-fluid temperature difference was not less than the uncertainty of the temperature measurements at the maximum Reynolds number of 2 300.

To prevent heat losses to the environment, the flow-calming section, inlet section, test section, mixers and connecting tubes were insulated using insulation with a thermal conductivity of 0.034 W/mK. The thickness of the insulation around the test section was 60 mm and the

maximum heat loss was estimated with one-dimensional heat transfer calculations to be less than 2%.

3. Numerical modelling

Numerical simulations were conducted using ANSYS Fluent 19.2. The following two assumptions were made for the mathematical description of the flow: (1) steady flow and (2) laminar flow. Based on these assumptions, the following governing equations describe the flow:

Continuity equation,

$$\frac{\partial u_i}{\partial x_i} = 0 \tag{1}$$

Momentum equation,

$$\rho u_j \frac{\partial u_i}{\partial x_j} = -\frac{\partial P}{\partial x_i} + \frac{\partial}{\partial x_j}\left(\mu \frac{\partial u_i}{\partial x_j}\right) + \rho g_i \tag{2}$$

Energy equation,

$$\rho u_i \frac{\partial (C_p T)}{\partial x_i} = \frac{\partial}{\partial x_i}\left(k \frac{\partial T}{\partial x_i}\right) \tag{3}$$

where u_i is the velocity vector, ρ is the density, P is the static pressure, x_i is the Cartesian coordinates, μ is the dynamic viscosity, g is the gravitational acceleration, T is the static temperature and C_p is the specific heat.

On the walls, no-slip boundary conditions prevailed for the momentum equation, while a constant heat flux boundary condition was assumed for the energy equation. A uniform velocity and temperature of 20 °C (293 K) were specified at the inlet, while a pressure outlet condition was specified at the outlet of the tube.

The SIMPLE (semi-implicit method for pressure-linked equations) technique was used as the Navier-Stokes solver [43]. For discretising the convective terms, a second-order accurate upwind scheme [44] was used. The discretised equations were then solved iteratively in a double precision solver. The convergence criteria for continuity, momentum and energy were set at 10^{-4}, 10^{-5} and 10^{-7}, respectively [45], which is ten times lower than the default settings.

Table 1: Grid independence study (*Re* = 600, upward flow, 2 kW/m^2)

	Total number of nodes	*Nu* (upward flow)	*Nu* (downward flow)
Grid 1	2 977 235	4.3566	4.3597
Grid 2	3 157 999	4.3723	4.3649
Grid 3	2 788 966	4.3730	4.3681

A structured grid distribution was created and a grid independence study was conducted in which the basic parameters such as the Nusselt number were obtained and compared. The grid independence study results are given in Table 1 and Grid 3, consisting of 2 788 966 nodes, provided sufficient accuracy and was used for this study.

4. Data reduction

The data reduction method was fully reported in Meyer *et al.* [39], but for the sake of completeness it is summarised in this paper. A linear equation was used to obtain the fluid temperatures at different locations along the tube length. The fluid inlet temperature, T_i, and outlet temperature, T_o, were measured using two Pt100 probes:

$$T(x) = T_i + \frac{(T_o - T_i)}{L} x \tag{4}$$

The above assumption of a linear variation in the bulk fluid temperature was used, because the test section was subjected to a constant heat flux boundary condition. Using Eq. (4), the bulk fluid temperature in the fully developed flow section was calculated at x = 3.92 m ($T_{b,FD}$ in Fig. 2).

The correlations of Popiel and Wojtkowiak [46] were used to calculate the fluid properties such as densities, ρ, viscosities, μ, thermal conductivity, k, specific heat, C_p, thermal expansion coefficient, β, and Prandtl number, Pr, at the bulk fluid temperature in the fully developed section.

The Reynolds numbers were calculated as:

$$Re = \frac{4\dot{m}}{\pi D_i \mu} \tag{5}$$

The effective heat transfer rates, $\dot{Q}_f$, were determined using the mass flow rates, $\dot{m}$, and the difference between the outlet and inlet temperatures:

$$\dot{Q}_f = \dot{m} C_p (T_o - T_i) \tag{6}$$

An energy balance error, eb, was used to determine the heat transfer efficiency of the electrical energy supplied, $\dot{Q} = I \times \Delta V$:

$$eb = \left[\frac{\dot{Q} - \dot{Q}_f}{\dot{Q}}\right] \times 100 \tag{7}$$

The heat flux, $\dot{q}_f$, was calculated as:

$$\dot{q}_f = \frac{\dot{Q}_f}{\pi D_i L} \tag{8}$$

The heat transfer rate to the fluid, $\dot{Q}_f$, was used to calculate the heat flux, because the electrical power to the system was predominantly higher than the actual heat transfer to the water, due to the heat loss from the test section. The calculated average energy balance error was found to be 2.7% and this was well in agreement with the theoretically calculated heat loss, which occurred as a result of the low thermal conductivity of the insulation material.

The local heat transfer coefficient at a distance *x* was calculated as:

$$h(x) = \frac{\dot{q}_f}{T_s(x) - T(x)} \tag{9}$$

where $T(x)$ and $T_s(x)$, were the mean fluid and inner surface temperatures at a distance *x* from the test section inlet. As the thermal conductivity of the copper test section was very high (401 W/mK), the thermal resistance across the tube wall was negligible [10]. The surface temperatures measured on the outside of the test section could therefore be used as the surface temperatures on the inside of the test section.

The local Nusselt numbers were calculated as:

$$Nu(x) = \frac{h(x)D_i}{k} \tag{10}$$

The average fully developed Nusselt numbers between x = 3.47 m (station 16) and x = 4.52 m (station 21) were calculated using the average of the local Nusselt numbers at the last six measuring thermocouples.

Similarly, the Grashof number, *Gr*, was:

$$Gr = \frac{g\beta\rho^2\big(T_s(x) - T(x)\big){D_i}^3}{\mu^2} \tag{11}$$

The average fully developed value of the Grashof number was determined using the values from the last six measurements.

5. Uncertainties

A confidence level of 95% was used to determine the uncertainties [47] and the details of the uncertainty analysis are given in Bashir *et al*. [40]. For the uncertainty analyses of this paper, the manufacturer instrumentation errors were used as the fixed errors and two times the standard deviation of 400 data points were used as the random errors. The Reynolds number uncertainties were approximately 1.5% for Reynolds numbers greater than 700 and increased to 4% as the Reynolds number was decreased to 400. For Reynolds numbers less than 400, the uncertainties increased significantly to a maximum uncertainty of 7%. The Reynolds number uncertainties were not significantly affected by the heat flux or flow direction.

At a heat flux of 2 kW/m^2, the average Nusselt number uncertainty was 4% and increased to 6% as the Reynolds number was decreased. At the lowest heat flux of 1 kW/m^2, the average Nusselt number uncertainty increased to 7%, due to the smaller surface-fluid temperature differences.

6. Validation

The full validation of the experimental set-up and data reduction method for both heat transfer and pressure drop can be found in Bashir *et al*. [40]. Only a summary of the heat transfer validation is presented in this paper, because the same experimental set-up and test section were used. The local Nusselt numbers at a Reynolds number of approximately 1 050 and heat flux of 4 kW/m^2, for both upward and downward flows, compared very well with the correlation of Shah and London [48], with an average deviation of 4% and maximum deviation of 8%. The flow was fully developed along the tube length from x/D = 416 [39], and the local Nusselt numbers converged to theoretical forced convection Nusselt number 4.36 with a maximum deviation of 4.7%.

7. Results

Fig. 3 contains the experimental and numerical fully developed Nusselt numbers as a function of Reynolds number for upward and downward flow at different heat fluxes. The experimental and numerical results are compared at a heat flux of 2 kW/m^2 in Fig. 3(a). Fig. 3(b) compares the experimental results at different heat fluxes, while the numerical results at different heat fluxes are compared in Fig. 3(c). The circle and square markers represent the upward and downward results, respectively, while the filled and empty markers represent the experimental and numerical results, respectively.

Fig. 3(a) indicates that there is in general very good agreement between the experimental and numerical results. Similar to the results obtained by Bashir *et al*. [40], the Nusselt numbers of both upward and downward flow increased with an increase in Reynolds number for Reynolds numbers greater than approximately 1 000. Therefore, the fully developed forced convection Nusselt numbers were not constant at 4.36. Bashir *et al*. [40] explained that this deviation from the constant property Nusselt number of 4.36 was generally due to changes in fluid properties, caused by changes in temperature either due to changes in heat flux or mass flow rate.

Between Reynolds numbers of approximately 250 to 1 000 and 600 to 1 000 for upward and downward flow, respectively, the Nusselt numbers remained approximately constant at 4.36. For upward flow, as the Reynolds number was decreased below 250 and approached 0 (no-flow condition), the Nusselt numbers decreased significantly from 4.36 and approached a Nusselt number of approximately 1, which corresponded to the Nusselt number for pure conduction heat transfer. For downward flow, this change from the forced convection Nusselt number of 4.63 to the pure conduction Nusselt number of 1 started at a higher Reynolds number of approximately 600.

A similar trend of increasing Nusselt numbers with increasing Reynolds numbers was found by Manay *et al*. [1], who studied assisting and opposing flow in minichannels between

Reynolds numbers of 20 and 60. The same trend was also observed by Sudo *et al*. [30], who investigated assisting and opposing flow in rectangular minichannels. As the Reynolds numbers was decreased, the Grashof number increased and free convection effects increased. The expected trend would be that the Nusselt numbers would increase with increasing free convection effects, similar to the results obtained by Mohammad and Salman [28, 29] in short vertical tubes (with a relatively large diameter of 30 mm), as well as by Meyer and Everts [10] and Everts and Meyer [9, 15, 49], who investigated mixed convective conditions in horizontal tubes. However, the results in Fig. 3 indicate that the Nusselt numbers decreased with increasing Grashof number (thus decreasing Reynolds number).

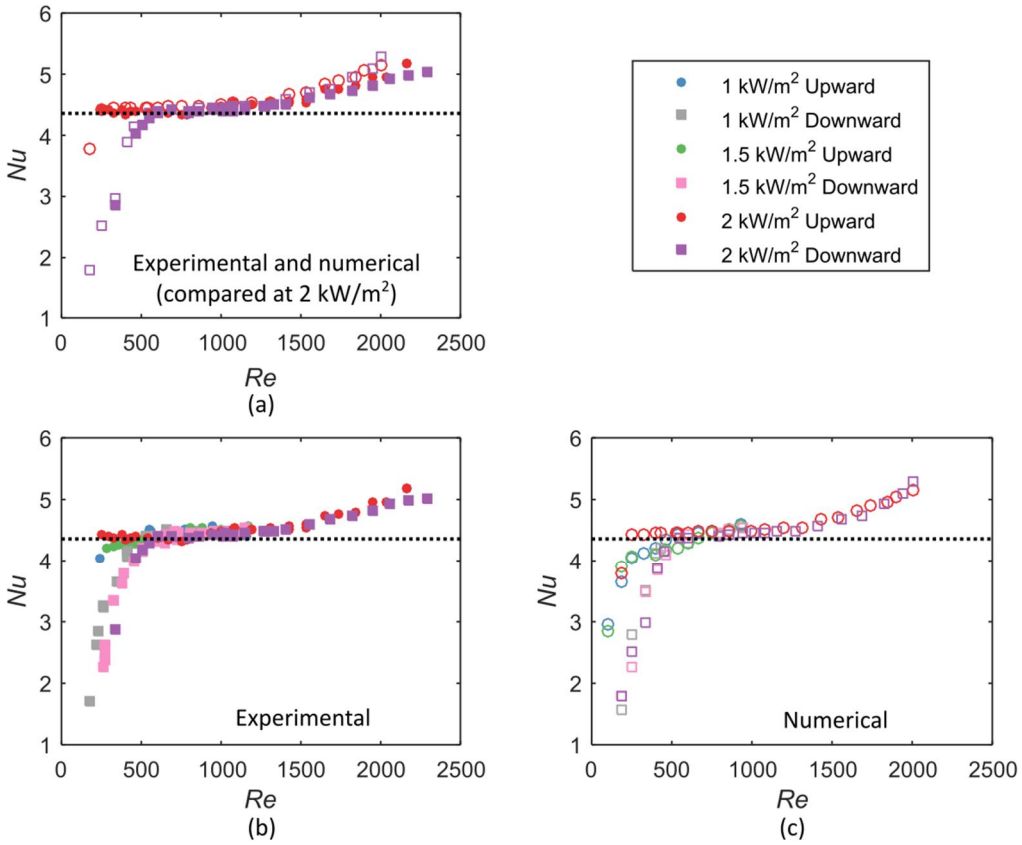

Fig. 3: Nusselt number as a function of Reynolds number for (a) upward and downward flows at a heat flux of 2 kW/m^2, (b) experimental results of all heat fluxes for upward and downward flows, and (c) numerical simulation results of all heat fluxes for upward and downward flows. The circle and square markers represent the upward and downward flow results, respectively, while the filled and empty markers represent the experimental and numerical results, respectively.

From Fig. 3 it follows that forced convection conditions existed for Reynolds numbers greater than 250 and 600 for upward and downward flow, respectively, because there was no significant difference between the Nusselt numbers of upward and downward flow. Although the theoretical Nusselt number is 4.36, this Nusselt number cannot be true for all Reynolds numbers. A Nusselt number of 1 would be expected at a Reynolds number of zero, in the absence of any free convection effects, because the heat transfer would then be by conduction only. As the Reynolds number is increased slightly above zero, heat transfer is no longer by conduction only and the contribution of convection heat transfer (due to the velocity of the fluid) causes the Nusselt numbers to increase. In the absence of any free convection effects,

the Nusselt numbers are therefore expected to gradually increase with increasing Reynolds number up to a Nusselt number of 4.36, when heat transfer by convection dominates heat transfer by conduction.

However, as these Reynolds numbers remain relatively low (below 600), the magnitude of free convection effects, in the presence of gravity, can be significant compared with the low fluid velocities. This explains the significant difference between the results for upward and downward flow in Fig. 3 for Reynolds numbers less than 600. Fig. 3(a) indicates that at a fixed Reynolds number, for example $Re = 400$, the Nusselt numbers for upward flow were always greater than for downward flow when free convection effects were significant ($Re < 600$). This is as expected and in good agreement with results of previous investigations [1, 19, 24, 29, 30, 37, 38]. For upward flow, free convection effects act in the same direction as the flow and therefore enhance heat transfer, while for downward flow, free convection effects act in the opposite direction as the flow and therefore adversely affect the heat transfer, compared to forced convection conditions with constant fluid properties [38].

It can therefore be postulated that in the absence of any free convection effects, the increasing Nusselt numbers with increasing Reynolds number between Reynolds numbers of zero and approximately 600, will fall in between the results of the upward and downward flow in Fig. 3. For these pure forced convection conditions, the Reynolds number at which the Nusselt number approaches the theoretical Nusselt number of 4.36, can thus also be expected to be between Reynolds numbers of 250 (for upward flow) and 600 (for downward flow). This is schematically summarised in Fig. 4. The solid black line represents forced convection conditions, while the blue, green and red lines represent upward (solid lines) and downward (dotted lines) flow with increasing Grashof numbers (thus increasing heat fluxes).

Similar trends were obtained with different heat fluxes (1 kW/m^2, 1.5 kW/m^2 and 2 kW/m^2) in Fig. 3(b) and (c). When comparing the results of the different heat fluxes, it follows that the heat flux had a small influence on the Reynolds numbers at which opposing and assisting flow become significant. From Fig. 3(b) it follows that the Reynolds numbers at which assisting flow became significant were 552, 462, and 253 for heat fluxes of 1 kW/m^2, 1.5 kW/m^2 and 2 kW/m^2. Furthermore, opposing flow became significant at Reynolds numbers of 525, 598 and 604 for heat fluxes of 1 kW/m^2, 1.5 kW/m^2 and 2 kW/m^2. A possible reason for these small differences, especially for downward flow, is that the three heat fluxes were relatively close to each other. However, these changes in Reynolds number were noteworthy, because it was more than the corresponding Reynolds number uncertainties.

It therefore follows from Fig. 3 that as the heat flux is increased, the increased free convection effects cause the Reynolds numbers at which assisting flow becomes significant to decrease, while the Reynolds numbers at which opposing flow becomes significant to increase. The changes in Reynolds number due to free convection effects were also greater for upward flow than for downward flow. Free convection effects can be quantified in terms of the Grashof number (Eq. (11)), which is a function of the surface-fluid temperature difference, as well as a strong function of the fluid properties (density and viscosity). When the heat flux is increased

by a factor of two, the surface-fluid temperature difference might increase proportionally, but the changes in fluid properties will not be proportional, which explains why the Grashof numbers do not increase proportionally. This explains why the changes in Reynolds numbers were not proportional with heat flux. Furthermore, for upward flow, free convection effects act in the same direction as the flow, while it acts in the opposite direction when the flow is downward. Therefore, free convection effects had a greater influence on the Reynolds numbers of assisting flow than of opposing flow.

As schematically summarised in Fig. 4, an increase in free convection effects (blue to red solid and dotted lines) therefore cause the Nusselt numbers to move further away from the postulated forced convection line, which is represented by the solid black line. Furthermore, the gradient of the Nusselt numbers lines as a function of Reynolds number became steeper with increasing free convection effects.

Furthermore, three distinct regions can be identified. At Reynolds numbers less than approximately 600, assisting and opposing flow is significant, therefore the Nusselt numbers is a function of the Reynolds number, Grashof number and Prandtl number. Between Reynolds numbers of approximately 600 and 1 000, free convection effects were suppressed by the velocity of the fluid. The Nusselt numbers remained constant at 4.36 and were independent of Reynolds number, Grashof number and Prandtl number. Similar to the findings of Bashir *et al.* [40], the Nusselt numbers increased with increasing Reynolds number for Reynolds numbers greater than 1 000, but were independent of Grashof number and Prandtl number.

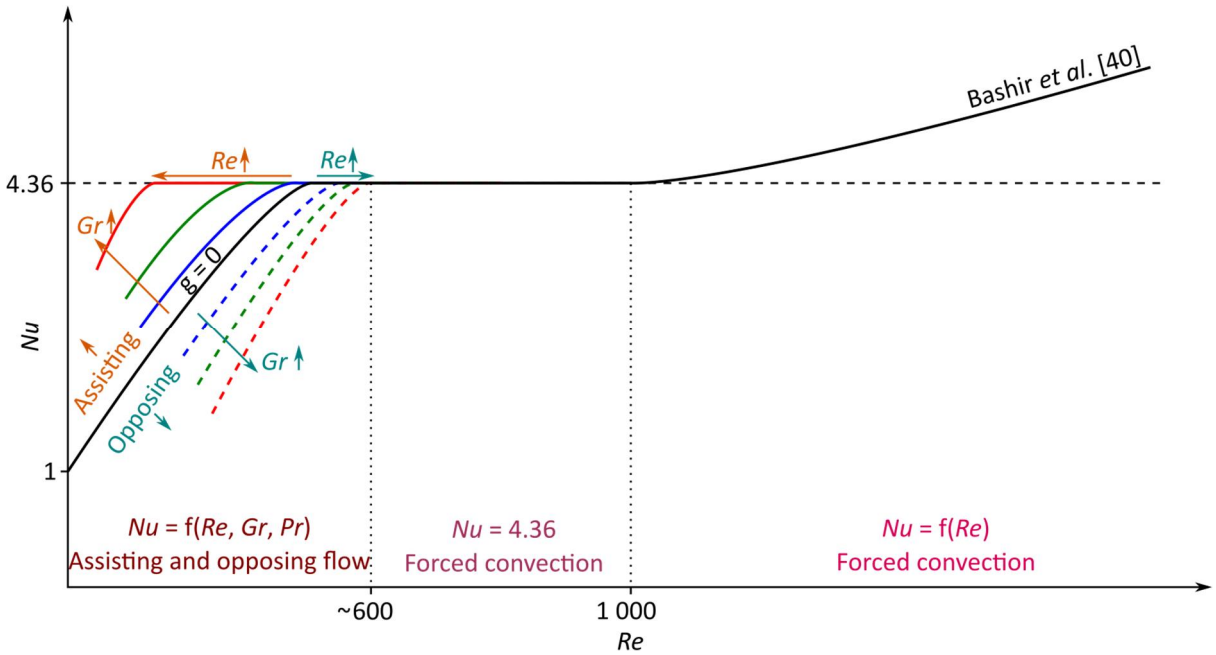

Fig. 4: Schematic summary indicating the effects of assisting and opposing flow on the fully developed forced convection Nusselt numbers as a function of Reynolds. The solid and dotted lines represent upward and downward flow, respectively. Blue, green and red indicates increased free convection effects.

To gain a better understanding of the flow characteristics of opposing and assisting flow, the axial velocity profiles as a function of dimensionless radial distance (r/D) at x/D = 833 are

compared for different Reynolds numbers (250, 500 and 900) at a constant heat flux of 2 kW/m^2 in Fig. 5. The circle and square markers represent the upward and downward numerical results, respectively, while the solid and dotted lines represent the upward and downward theoretical $\left(u(r) = 2V_{avg}\,(1 - r^2/R^2)\right)$ results, respectively.

As expected, the velocity of the fluid in contact with the surface of the tube was essentially zero and increased towards the centreline of the tube. Furthermore, the maximum axial velocity also increased with increasing Reynolds number. The solid and dotted lines indicate that the maximum of the theoretical velocity profile was located in the centre of the tube for both upward and downward flows. However, the numerical results indicate that the shape of the velocity curve was influenced by the flow direction. There was a significant difference between the theoretical and numerical results and the difference increased from approximately 20% at a Reynolds number of 250, to 30% at a Reynolds number of 900, for upward flow. For downward flow, the difference was even more (30%-40%) because the velocity profile was flatter near the centreline of the tube. Similar trends were also observed in the results of Manay *et al*. [1], however, the authors did not explain the flow physics behind these trends.

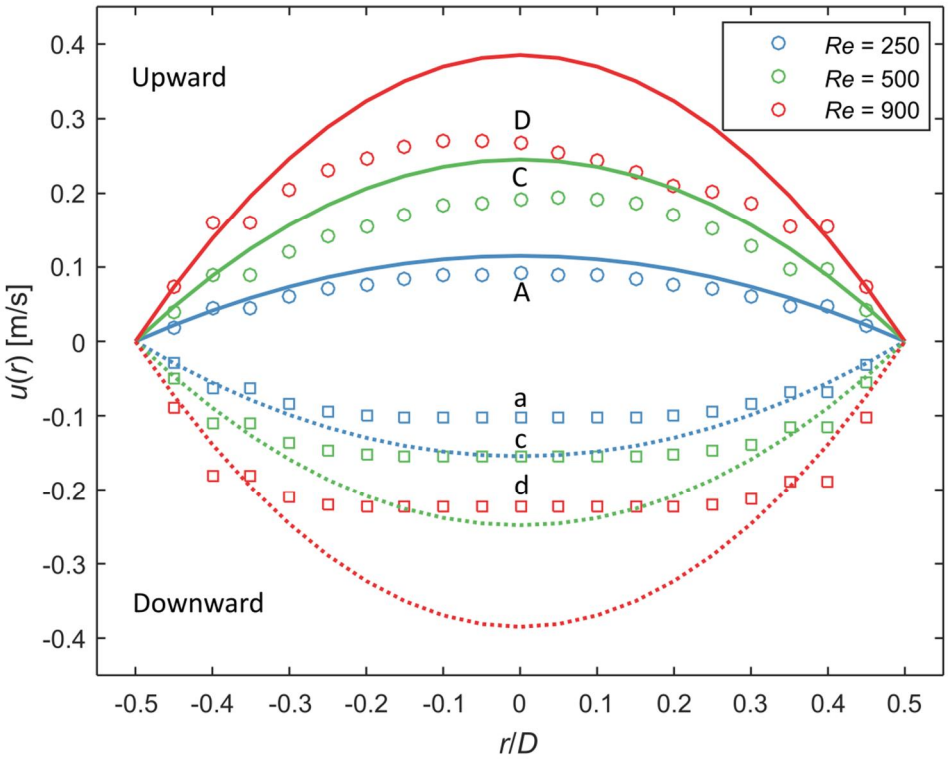

Fig. 5: Axial velocity profile for upward and downward flow at *x/D* = 833, as a function of dimensionless radial distance (*r/D*), for different Reynolds numbers and a constant heat flux of 2 kW/m^2. The circle and square markers represent the upward and downward numerical results, respectively, while the solid and dotted lines represent the upward and downward theoretical results, respectively.

To investigate the influence of the velocity profile on the heat transfer inside the tube, Fig. 6 contains the Nusselt numbers as a function of Reynolds number together with the temperature contour plots (Fig. 6(a)) and streamlines in the transverse plane (Fig. 6(b)), for upward and downward flow at a dimensionless axial distance of *x/D* = 883 and a constant heat flux of

2 kW/m^2. From Fig. 5 and Fig. 6(a) it follows that for upward flow, the differences between the theoretical and numerical velocity profiles did not have a significant influence on the Nusselt numbers for Reynolds numbers between 250 and 900, because they remained within 3% of the theoretical Nusselt number of 4.36. At a Reynolds number of 250, the temperature contour plot shows that the temperature decreased radially from the surface to the centre of the tube. However, as the Reynolds number increased to 500 and 900, the temperature contour plots show that the temperature distribution became more distorted with increasing Reynolds number. This led to significant temperature gradients inside the cross section and increased the Nusselt numbers above the theoretical Nusselt number of 4.36.

It also follows from Fig. 5 that for upward flow, the peak of the velocity profile was no longer in the centre of the tube, but moved towards the surface of the tube. The streamlines in Fig. 6(a) indicate that two vortices existed inside the cross-section of the tube. As the Reynolds number was increased, these vortices moved towards the surface of the tube. However, free convection effects also caused these vortices to rotate in a radial direction. This explains why the peaks of the velocity profiles in Fig. 5 alternated between the left and right side of the graph as the Reynolds number was increased.

For downward flow, the temperature contour plots in Fig. 6(a) show that the flatter velocity profile at a Reynolds number of 250 (Fig. 5) led to a thinner high temperature region near the surface of the tube, while a greater portion in the centre of the tube contained fluid at a lower temperature. Similar to upward flow, the temperature contour plots show that the temperature distribution became distorted with increasing Reynolds number. Although the velocity profile (Fig. 5) for downward flow was flatter than for upward flow, the streamlines in Fig. 6(b) indicate that two vortices existed inside the cross-section that also moved towards the surface of the tube as the Reynolds number was increased. Unfortunately, due to the significant free convection effects at a Reynolds number of 250, it was not possible to obtain clear streamlines at this Reynolds number. According to Hanratty *et al*. [20], the flow might become unstable and backflow might occur for $Gr/Re > 49.2$, which was the case in Fig. 6. For upward flow, backflow was only expected for $Gr/Re > 122$, which is an order of magnitude more than for the results in Fig. 6.

The streamlines in Fig. 6(b) indicate that before assisting and opposing flow became significant and the Nusselt number was approximately 4.36, such as at a Reynolds number of 250 for upward flow (point A) and 500 for downward flow (point c), the streamlines were similar and two vortices existed near the centre of the tube. Furthermore, when free convection effects were completely suppressed by the velocity of the fluid, such as at Reynolds numbers of 900 (points D for upward flow and d for downward flow), the streamlines were again similar and therefore the Nusselt numbers were also approximately the same. Because the tube was heated, the fluid properties changed with temperature, which led to free convection effects in the presence of gravity. However, the velocity of the fluid was sufficient to restrict these free convection effects to a region near the surface of the tube. This led to a greater temperature gradient in the cross-section as well as increased Nusselt numbers.

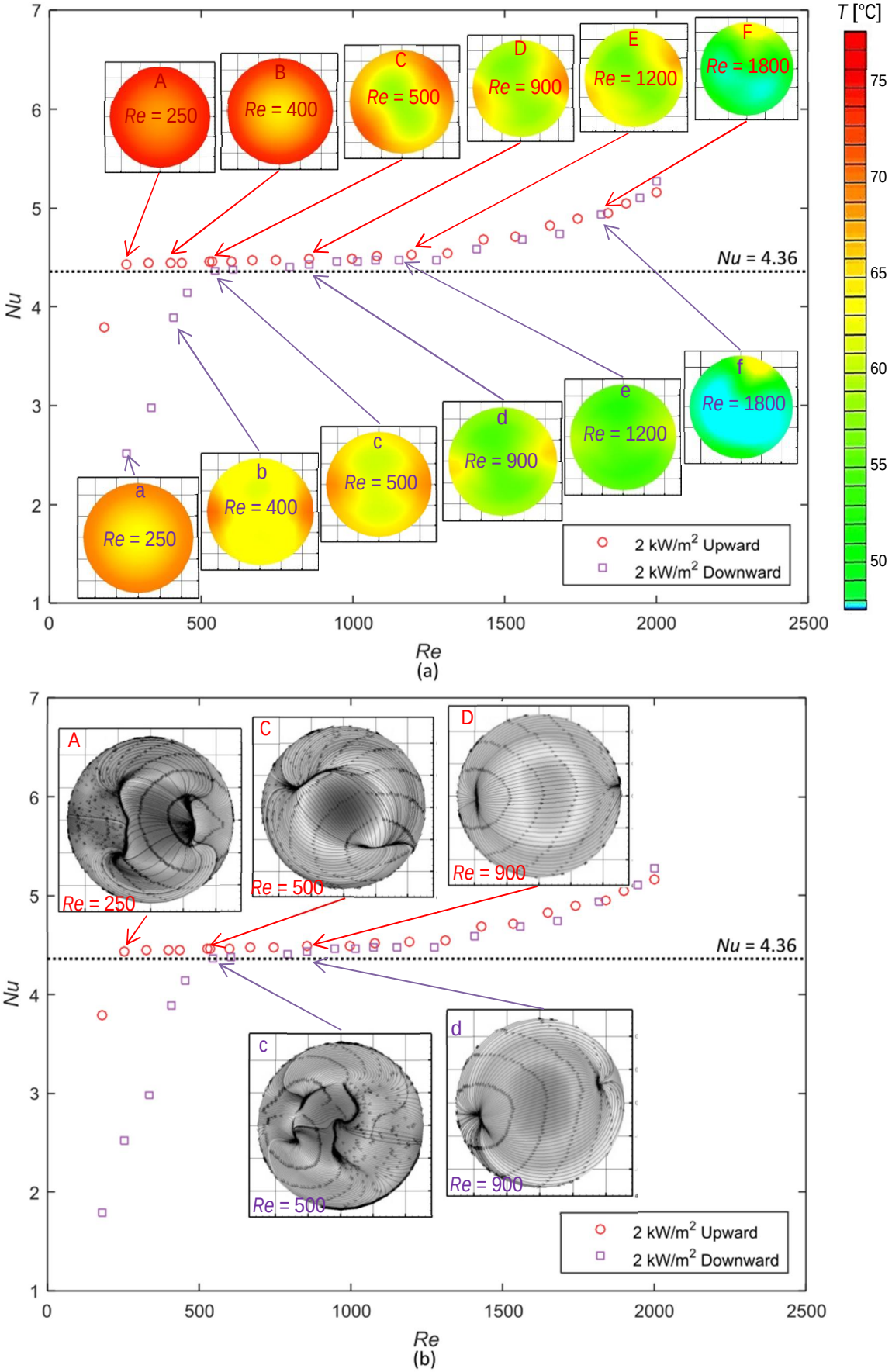

Fig. 6: Nusselt numbers as a function of Reynolds number with (a) temperature contour plots and (b) streamlines in the transverse planes for upward and downward flows at a dimensionless axial distance of *x/D* = 883 and a constant heat flux at 2 kW/m^2.

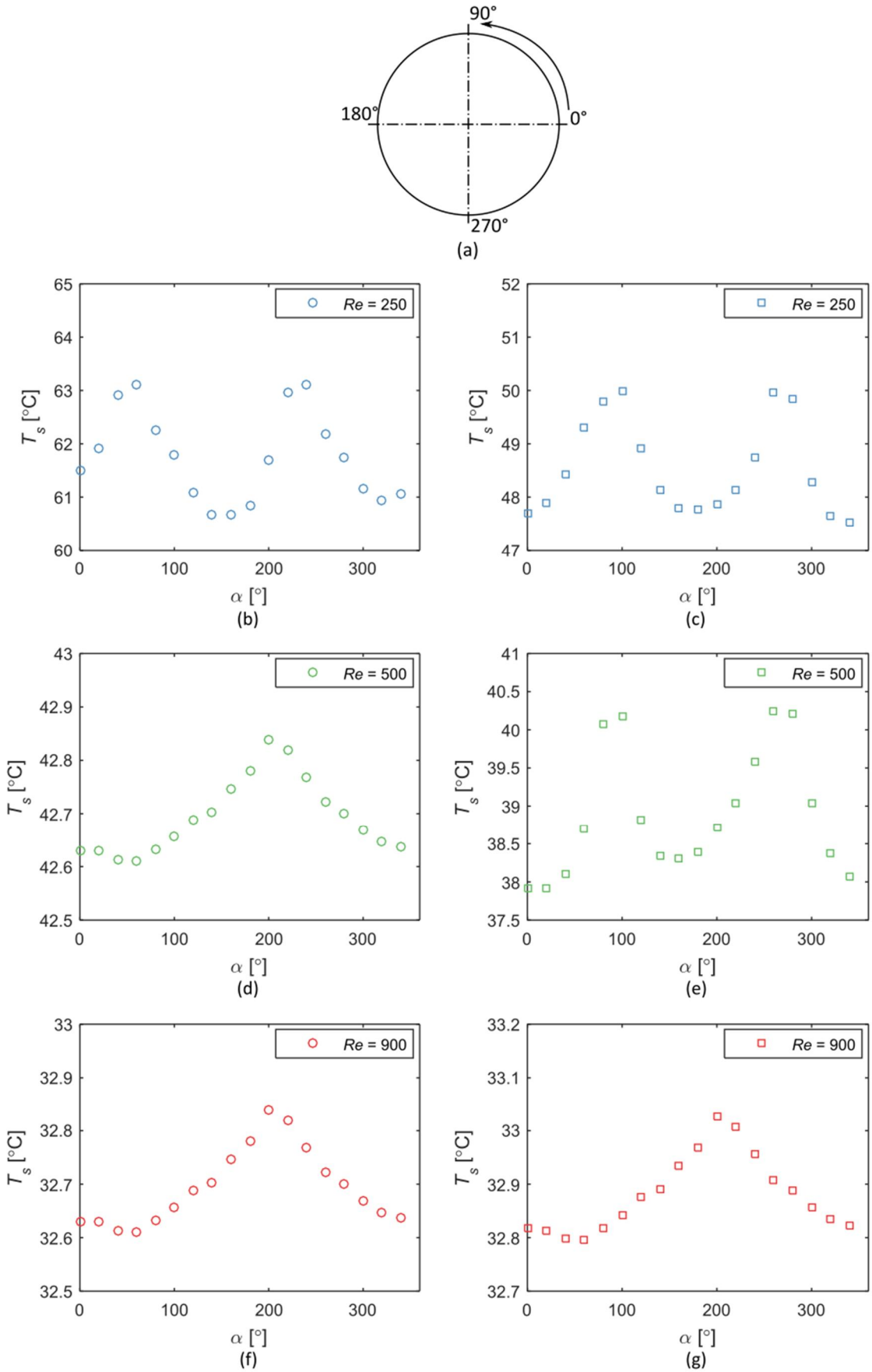

Fig. 7: Peripheral wall temperature as a function of angle (using the convection in (a)) at x/D = 883 and a heat flux of 2 kw/m^2 for different Reynolds numbers. The circle ((b), (d) and (f)) and square ((c), (e) and (g)) markers represent upward and downward flow, respectively.

Fig. 7 contains the peripheral wall temperatures as a function of angle (using the convention in Fig. 7(a)) at x/D = 883 and a constant heat flux of 2 kW/m^2 for different Reynolds numbers. The circle ((b), (d) and (f)) and square ((c), (e) and (g)) markers represent upward and downward flow, respectively. Every small fluctuation in Fig. 7 corresponds to a small change in the temperature gradient on the surface of the tube. Although it was not clear from the temperature contour plots in Fig. 6(a), due to the temperature scale that was used, it follows from Fig. 7 that free convection effects led to greater peripheral temperature variations at low Reynolds numbers. As indicated by the streamlines in Fig. 6(b), these greater temperature variations were caused by the increased stream-wise vortices. The vortices were effective in assisting with the distribution of heat from the surface to the centre of the tube, however, as the vortices were not symmetrical, peaks in the peripheral temperature profiles existed. It is interesting to note from Fig. 7(b), (c) and (e) that the peaks and troughs occurred 180° apart. The reason for this being the two vortices that were opposite one another existed inside the cross-section of the tube.

When comparing Fig. 7(d), (f) and (g) with the Nusselt numbers in Fig. 6, it follows that once free convection effects were suppressed and forced convection conditions dominated (the Nusselt numbers were approximately 4.36), the peripheral temperature profile became constant. A single peak was observed at 200° and a single trough at 60°. The location of the peak and the trough did not rotate radially. This is most probably because forced convection conditions existed and free convection effects, which could cause the rotation, were suppressed by the axial velocity of the fluid.

Bashir *et al*. [40] developed a forced convection Nusselt number correlation that accounts for the variations in fluid properties. However, this correlation is only valid for Reynolds numbers greater than 1 000. It follows from Fig. 3 that for Reynolds numbers less than 250 and 600 for upward and downward flow, respectively, the Nusselt numbers were no longer constant at 4.36. Assisting and opposing flow due to free convection effects had a significant influence on the Nusselt numbers. The following correlation was developed to calculate the Nusselt numbers for upward flow:

$$Nu = 1.72\left(RePr^{\frac{1}{3}}Gr^{-0.3}\right)^{0.21} \tag{12}$$

Eq. (12) was valid for $100 \leq Re \leq 300$, $1\,020 \leq Gr \leq 1\,550$ and $2.1 \leq Pr \leq 4.9$, and was able to predict all the data of this study within 3.5%.

The following correlation was developed for downward flow, where free convection effects acted in the opposite direction as the forced flow:

$$Nu = 0.662\left(RePr^{\frac{1}{3}}Gr^{-0.3}\right)^{0.4} \tag{13}$$

Eq. (13) was valid for $180 \leq Re \leq 650$, $866 \leq Gr \leq 18\,607$ and $2.7 \leq Pr \leq 5.6$, and was able to predict all the data of this study within 2.5%.

By making use of the method of Churchill and Usagi [50], Eqs. (12) and (13) were combined with the correlation of Bashir *et al*. [40], to obtain single correlations for upward and downward flow, respectively, that are valid for Reynolds numbers between 100 and 3 000 and Prandtl numbers between 2.1 and 8.1:

$$Nu = (Nu_1^{-10} + Nu_2^{-10})^{-0.1} \quad (14)$$

where Nu_1 can be substituted with either Eqs. (12) and (13) for upward and downward flow, respectively, and Nu_2 can be substituted with the correlation of Bashir *et al*. [40]:

$$Nu_2 = 4.36 + 5.36 \times 10^{-9} Re^{2.39} \quad (15)$$

Eq. (15) is valid for $600 \leq Re \leq 3\,000$, $728 \leq Gr \leq 24\,426$ and $3.5 \leq Pr \leq 8.1$. Although the exponent of -10 used in Eq. (14) might seem high (exponents of 3 and 4 are often used), this was required to account for the sudden decrease in Nusselt number with decreasing Reynolds number when opposing and assisting flow became significant. The use of Eqs. (12)-(15) is schematically summarised in Fig. 8. Eq. (14) performed very well and was able to predict the upward and down results with average deviations of 5%.

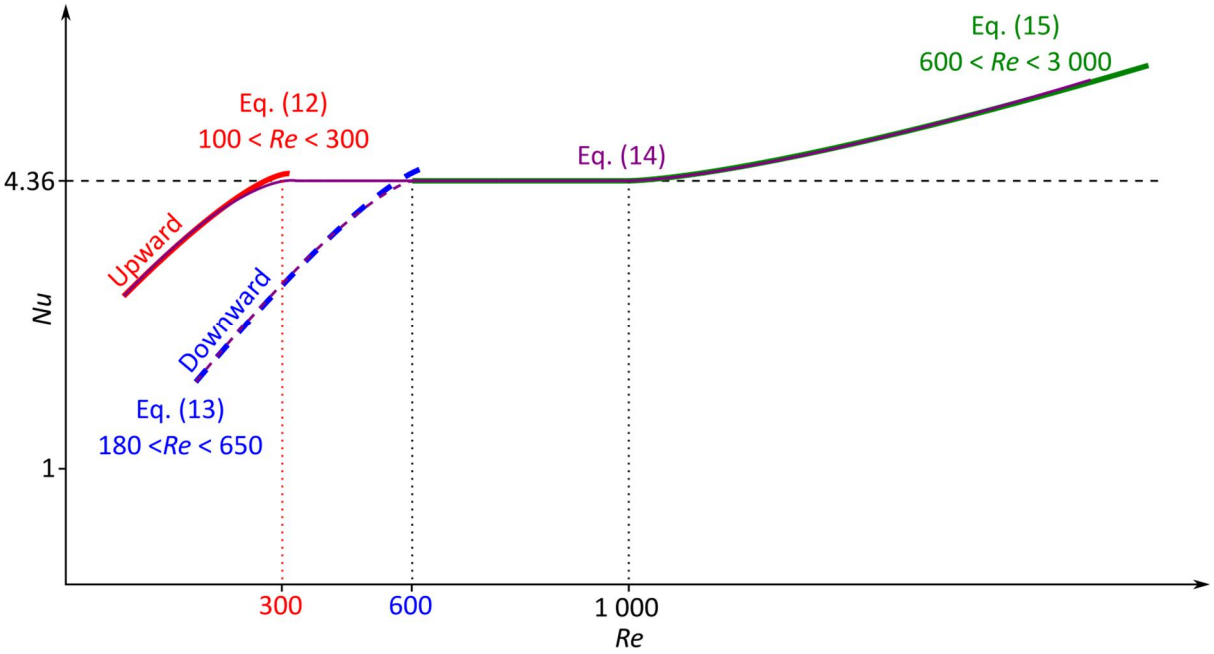

Fig. 8: Schematic summary of the use of Eqs. (12)-(15) for upward (solid lines) and downward (dotted lines) laminar flow.

8. Conclusions

This study experimentally and numerically investigated the heat transfer characteristics of laminar fully developed upward and downward flow through vertical tubes. Experiments were conducted between Reynolds numbers of 180 and 2 300 at three different constant heat fluxes

of 1, 1.5 and 2 kW/m^2, using water as the test fluid. The inner-tube diameter was 5.1 mm and the heated length-to-diameter ratio was 886. Numerical simulations were conducted at the same Reynolds numbers and heat fluxes using ANSYS Fluent and the numerical results compared well with the experimental results.

It was found that when the Reynolds numbers were greater than approximately 250 and 600 for upward and downward flow, respectively, forced convection conditions existed and there was no significant difference between the results of the upward and downward flow at different heat fluxes. As the Reynolds number was decreased below 250 and 600 for upward and downward flow, respectively, free convection effects were no longer suppressed by the velocity of the fluid, therefore assisting and opposing flow became significant. Because free convection effects acted in the same direction as the fluid flow for upward flow, heat transfer was enhanced, therefore the Nusselt numbers were greater than for forced convection conditions. The opposite was true for downward flow, because the heat transfer was impaired by the free convection effects that acted in the opposite direction as the fluid flow. As the heat flux was increased, free convection effects increased. This caused the Reynolds number at which assisting flow became significant to decrease, while the Reynolds number at which opposing flow became significant, increased. Furthermore, the gradient of the Nusselt numbers as a function of Reynolds number of assisting and opposing flow became steeper. The result was thus that the Nusselt numbers moved further away from the forced convection Nusselt numbers.

Correlations were developed to determine the Nusselt numbers for assisting ($Re < 300$) and opposing ($Re < 650$) flow and the correlations were able to predict the results of this study within 3.5% and 2.5%, respectively. These correlations were also combined with an existing laminar forced convection correlation in literature to obtain single correlations for upward and downward flow, respectively, that are valid for the entire laminar flow regime. As these correlations are limited to using water as the test fluid through smooth tubes, future work can include the investigations of different heat transfer fluids and surface roughness on the heat transfer characteristics of assisting and opposing flow in vertical tubes.

Acknowledgements

The funding obtained in South Africa from the National Research Foundation (Grant Number: 116623), Department of Science and Innovation (DSI), and University of Pretoria, as well as the support and resources of the Centre for High Performance Computing (CHPC), are acknowledged and duly appreciated.

CRediT authorship contribution statement

Marilize Everts: conceptualization, formal analysis, supervision, writing – original draft. Suvanjan Bhattacharyya: data curation, formal analysis, investigation, methodology, validation, writing – original draft. Abubakar I. Bashir: data curation, formal analysis, investigation, methodology, validation. Josua P. Meyer: conceptualization, funding acquisition, resources, supervision, writing – review and editing.

References

[1] E. Manay, E. Mandev, R.O. Temiz, Analysis of mixed convection heat transfer of nanofluids in a minichannel for aiding and opposing flow conditions, Heat Mass Transfer, 55(10) (2019) 3003-3015.
[2] Y.A. Cengel, A.J. Ghajar, Heat and Mass Transfer: Fundamentals and Applications, 5th ed., McGraw-Hill, 2015.
[3] J.H.I. Lienhard, J.H.V. Lienhard, A Heat Transfer Textbook, 3rd ed., Phlogiston Press, Cambridge, 2008.
[4] A. Bejan, Convection Heat Transfer, 4th ed., John Wiley & Sons, Hoboken, 2013.
[5] J.P. Holman, Heat Transfer, 9th ed., McGraw-Hill, New York, 2002.
[6] T.L. Bergman, A.S. Lavine, F.P. Incropera, D.P. De Witt, Fundamentals of Heat and Mass Transfer, 8th ed., Wiley, New York, 2017.
[7] R.K. Shah, A.L. London, Laminar Flow Forced Convection in Ducts: A Source Book for Compact Heat Exchanger Analytical Data, Academic Press, 1978.
[8] L.M. Tam, A.J. Ghajar, Effect of inlet geometry and heating on the fully developed friction factor in the transition region of a horizontal tube, Exp. Therm. Fluid Sci., 15(1) (1997) 52-64.
[9] M. Everts, J.P. Meyer, Heat transfer of developing and fully developed flow in smooth horizontal tubes in the transitional flow regime, Int. J. Heat Mass Transf., 117 (2018) 1331-1351.
[10] J.P. Meyer, M. Everts, Single-phase mixed convection of developing and fully developed flow in smooth horizontal circular tubes in the laminar and transitional flow regimes, Int. J. Heat Mass Transf., 117 (2018) 1251-1273.
[11] R. Siegel, E.M. Sparrow, T.M. Hallman, Steady laminar heat transfer in a circular tube with a prescribed wall heat flux, Applied Scientific Research, 7 (1958).
[12] G.A. Kemeny, E.V. Somers, Combined free and forced-convective flow in vertical circular tubes-experiments with water and oil, Journal of Heat Transfer, 84(4) (1962) 339-345.
[13] C.K. Brown, W.H. Gauvin, Combined free-and-forced convection: I. Heat transfer in aiding flow, The Canadian Journal of Chemical Engineering, 43(6) (1965) 306-312.
[14] B. Metais, E. Eckert, Forced, mixed, and free convection regimes, Journal of Heat Transfer, 86(2) (1964) 295-296.
[15] M. Everts, J.P. Meyer, Flow regime maps for smooth horizontal tubes at a constant heat flux, Int. J. Heat Mass Transf., 117 (2018) 1274-1290.
[16] M. Everts, Single-phase mixed convection of developing and fully developed flow in smooth horizontal circular tubes in the laminar, transitional, quasi-turbulent and turbulent flow regimes, PhD thesis, University of Pretoria, Pretoria, 2017.
[17] P.H. Newell, Jr., Laminar-flow heat transfer in horizontal tubes, PhD thesis, Massachusetts Institute of Technology, Boston, 1966.
[18] N. Galanis, A. Behzadmehr, Mixed convection in vertical ducts, in: 6th IASME/WSEAS International Conference on Fluid Mechanics and Aerodynamics (FMA'08), Rhodes, Greece, 2008.
[19] J.D. Jackson, M.A. Cotton, B.P. Axcell, Studies of mixed convection in vertical tubes, Int. J. Heat Fluid Flow, 10(1) (1989) 2-15.
[20] T.J. Hanratty, E.M. Rosen, R.L. Kabel, Effect of Heat Transfer on Flow Field at Low Reynolds Numbers in Vertical Tubes, Industrial & Engineering Chemistry, 50(5) (1958) 815-820.
[21] B.R. Morton, Laminar convection in uniformly heated vertical pipes, Journal of Fluid Mechanics, 8(2) (1960) 227-240.
[22] M. Iqbal, J.W. Stachiewicz, Influence of tube orientation on combined free and forced laminar convection heat transfer, Journal of Heat Transfer, 88(1) (1966) 109-116.

[23] R. Greif, An experimental and theoretical study of heat transfer in vertical tube flows, Journal of Heat Transfer, 100(1) (1978) 86-91.
[24] T.M. Hallman, Experimental study of combined forced and free laminar convection in a vertical tube, National Aeronautics and Space Administration, Cleveland, 1961.
[25] G.S. Barozzi, A. Dumas, M.W. Collins, Sharp entry and transition effects for laminar combined convection of water in vertical tubes, Int. J. Heat Fluid Flow, 5(4) (1984) 235-241.
[26] H. Mohammed, T. Yusaf, Heat transfer by mixed convection opposing laminar flow from the inside surface of uniformly heated inclined circular tube, in: Proceedings of 8th Biennial ASME Conference on Engineering Systems Design and Analysis, ESDA2006, 2006.
[27] H.A. Mohammed, Laminar mixed convection heat transfer in a vertical circular tube under buoyancy-assisted and opposed flows, Energy Conversion and Management, 49(8) (2008) 2006-2015.
[28] H.A. Mohammed, Y.K. Salman, Combined convection heat transfer for thermally developing aiding flow in an inclined circular cylinder with constant heat flux, Applied Thermal Engineering, 27(8-9) (2007) 1236-1247.
[29] H.A. Mohammed, Y.K. Salman, Heat transfer measurements of mixed convection for upward and downward laminar flows inside a vertical circular cylinder, Exp. Heat Transf., 21(1) (2008) 1-23.
[30] Y. Sudo, K. Miyata, H. Ikawa, M. Ohkawara, M. Kaminaga, Experimental study of differences in single-phase forced-convection heat transfer characteristics between upflow and downflow for narrow rectangular channel, Journal of Nuclear Science and Technology, 22(3) (1985) 202-212.
[31] M.M. Derakhshan, M.A. Akhavan-Behabadi, Mixed convection of MWCNT-heat transfer oil nanofluid inside inclined plain and microfin tubes under laminar assisted flow, Int. J. Therm. Sci., 99 (2016) 1-8.
[32] W.T. Lawrence, J.C. Chato, Heat-transfer effects on the developing laminar flow inside vertical tubes, Journal of Heat Transfer, 88(2) (1966) 214-222.
[33] K.C. Cheng, S.W. Hong, Effect of tube inclination on laminar convection in uniformly heated tubes for flat-plate solar collectors, Solar Energy, 13(4) (1972) 363-371.
[34] K.C. Cheng, S.W. Hong, Combined free and forced laminar convection in inclined tubes, Applied Scientific Research, 27(1) (1973) 19-38.
[35] A. Moutsoglou, Y.D. Kwon, Laminar mixed convection flow in a vertical tube, Journal of Thermophysics and Heat Transfer, 7(2) (1993) 361-368.
[36] Y.C. Su, J.N. Chung, Linear stability analysis of mixed-convection flow in a vertical pipe, Journal of Fluid Mechanics, 422 (2000) 141-166.
[37] J. Orfi, N. Galanis, Developing laminar mixed convection with heat and mass transfer in horizontal and vertical tubes, Int. J. Therm. Sci., 41(4) (2002) 319-331.
[38] M.W. Collins, Heat transfer by laminar combined convection in a vertical tube - predictions for water, in: Proceedings of the 6th International Heat Transfer Conference, Toronto, 1978, pp. 25-30.
[39] J.P. Meyer, A.I. Bashir, M. Everts, Single-phase mixed convective heat transfer and pressure drop in the laminar and transitional flow regimes in smooth inclined tubes heated at a constant heat flux, Exp. Therm. Fluid Sci., 109 (2019).
[40] A.I. Bashir, M. Everts, R. Bennacer, J.P. Meyer, Single-phase forced convection heat transfer and pressure drop in circular tubes in the laminar and transitional flow regimes, Exp. Therm. Fluid Sci., 109 (2019).
[41] H.A. Mohammed, Y.K. Salman, Combined natural and forced convection heat transfer for assisting thermally developing flow in a uniformly heated vertical circular cylinder, International Communications in Heat and Mass Transfer, 34(4) (2007) 474-491.

[42] M. Everts, J.P. Meyer, Laminar hydrodynamic and thermal entrance lengths for simultaneously hydrodynamically and thermally developing forced and mixed convective flows in horizontal tubes, Exp. Therm. Fluid Sci., (2020).
[43] S. Bhattacharyya, H. Chattopadhyay, A.C. Benim, Simulation of heat transfer enhancement in tube flow with twisted tape insert, Progress in Computational Fluid Dynamics, 17(3) (2017) 193-197.
[44] S. Bhattacharyya, H. Chattopadhyay, A.C. Benim, Computational investigation of heat transfer enhancement by alternating inclined ribs in tubular heat exchanger, Progress in Computational Fluid Dynamics, 17(6) (2017) 390-396.
[45] S. Bhattacharyya, H. Chattopadhyay, A. Guin, A.C. Benim, Investigation of Inclined Turbulators for Heat Transfer Enhancement in a Solar Air Heater, Heat Transfer Eng, 40(17-18) (2019) 1451-1460.
[46] C.O. Popiel, J. Wojtkowiak, Simple formulas for thermophysical properties of liquid water for heat transfer calculations [from O°C to 150°C], Heat Transfer Eng, 19(3) (1998) 87-101.
[47] P.F. Dunn, Measurement and Data Analysis for Engineering and Science, 2nd ed., CRC Press, United States of America, 2010.
[48] R.K. Shah, M.S. Bhatti, Laminar convective heat transfer in ducts, in: S. Kakaç, R.K. Shah, W. Aung (Eds.) Handbook of Single-Phase Convective Heat Transfer, John Wiley & Sons, New York, 1987, pp. 3.1-3.31.
[49] M. Everts, J.P. Meyer, Relationship between pressure drop and heat transfer of developing and fully developed flow in smooth horizontal circular tubes in the laminar, transitional, quasi-turbulent and turbulent flow regimes, Int. J. Heat Mass Transf., 117 (2018) 1231-1250.
[50] S.W. Churchill, R. Usagi, A general expression for the correlation of rates of transfer and other phenomena, AIChE Journal, 18(6) (1972) 1121-1128.